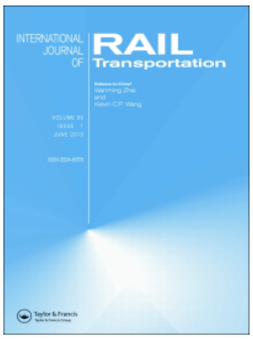

International Journal of Rail Transportation

ISSN: (Print) (Online) Journal homepage: https://www.tandfonline.com/loi/tjrt20

High-speed train–track–bridge dynamic interactions – Part I: theoretical model and numerical simulation

Wanming Zhai, He Xia, Chengbiao Cai, Mangmang Gao, Xiaozhen Li, Xiangrong Guo, Nan Zhang & Kaiyun Wang

To cite this article: Wanming Zhai, He Xia, Chengbiao Cai, Mangmang Gao, Xiaozhen Li, Xiangrong Guo, Nan Zhang & Kaiyun Wang (2013) High-speed train–track–bridge dynamic interactions – Part I: theoretical model and numerical simulation, International Journal of Rail Transportation, 1:1-2, 3-24, DOI: 10.1080/23248378.2013.791498

To link to this article: https://doi.org/10.1080/23248378.2013.791498

Published online: 29 May 2013.

International Journal of Rail Transportation, 2013
Vol. 1, Nos. 1–2, 3–24, http://dx.doi.org/10.1080/23248378.2013.791498

High-speed train–track–bridge dynamic interactions – Part I: theoretical model and numerical simulation

Wanming Zhai[a]*, He Xia[b], Chengbiao Cai[a], Mangmang Gao[c], Xiaozhen Li[d], Xiangrong Guo[e], Nan Zhang[b] and Kaiyun Wang[a]

[a]*Train and Track Research Institute, State Key Laboratory of Traction Power, Southwest Jiaotong University, Chengdu 610031, China;* [b]*School of Civil Engineering, Beijing Jiaotong University, Beijing 100044, China;* [c]*Railway Scientific Research and Development Centre, China Academy of Railway Sciences, Beijing 100081, China;* [d]*School of Civil Engineering, Southwest Jiaotong University, Chengdu 610031, China;* [e]*School of Civil Engineering, Central South University, Changsha 410075, China*

(*Received 20 December 2012; final version received 22 March 2013*)

This paper presents a framework to systematically investigate the high-speed train–track–bridge dynamic interactions, aiming to provide a method for analysing and assessing the running safety and the ride comfort of trains passing through bridges, which are critically important for the design of new high-speed railway bridges. Train–track–bridge interactive mechanism is illustrated. A fundamental model is established for analysing the train–track–bridge dynamic interactions, in which the vehicle subsystem is coupled with the track subsystem through a spatially interacted wheel–rail model; and the track subsystem is coupled with the bridge subsystem by a track–bridge dynamic interaction model. Modelling of each subsystem and each interactive relationship between subsystems are presented. An explicit–implicit integration scheme is adopted to numerically solve the equations of motion of the large non-linear dynamic system in the time domain. Computer simulation software named the train–track–bridge interaction simulation software (TTBSIM) is developed to predict the vertical and lateral dynamic responses of the train–track–bridge coupled system.

Keywords: train–track–bridge interaction; dynamic model; computer simulation; high-speed railway; bridge

1. Introduction

Train–bridge interaction is a classic railway dynamics topic that has been studied for quite some time. As operating speed of train has been steadily increased, a growing attention is paid to this topic. Early work on train–bridge interaction was generally conducted on bridges, focusing on the analytical low-frequency vibration responses of bridge and key factors contributing to train–bridge system resonance [1–3]. Around 1980s, substantial research results were obtained through studies on train–bridge interactions; examples include work [4–7] which were based on improvements of analytical models of trains and bridges. However, previous studies did not consider the influence of vibration of the track structure on train–bridge system dynamics. As a matter of fact, trains operate on the track structure; and the track structure is laid on bridge body. Therefore, train, track and bridge essentially form an integrated dynamic system, in which train and track are coupled by wheel–rail interactive relationship, and track and bridge are linked through track–

*Corresponding author. Email: wmzhai@swjtu.edu.cn

bridge interaction. It is rational to integrate train, track and bridge into an interactive system for further analysis. Based on this concept, Zhai in 1995 started to investigate the train–track–bridge system dynamics, which is also an extension from the vehicle–track coupled dynamics [8]. In 1997, a dynamic model of vertically coupled locomotive–track–bridge system was established based on a simply supported beam bridge, in which track vibration was included on the model for the first time [9]. This model was later applied to analyse and evaluate dynamic performance of two large bridges with slab track structures in China's first passenger transport special railway line, the Qinhuangdao–Shenyang line [10]. Zhai et al. further introduced a spatial coupled wheel–rail model into the system and extended the study to resolve both vertical and lateral dynamic interactions among train, track and bridge [11].

Meanwhile, other researchers have also conducted comprehensive work on the train–bridge interaction problems integrating the train, track and bridge as a single system. Cheng et al. [12] presented a type of vehicle–track–bridge element to investigate the two-dimensional (2D) interaction among a moving train, its supporting railway track structure and bridge structure. Such an element consists of mass–spring–damper systems as the vehicle model, an upper beam element as the rail model and a lower beam element as the bridge deck model. Biondi et al. [13] investigated the 2D dynamic interaction among a running train, a track structure and a supporting bridge resorting to the substructure technique. In the paper, the train was idealised as a sequence of identical vehicles moving at constant speed. Both the rails and the bridge were modelled as Bernoulli–Euler beams, while the ballast was characterised as a viscoelastic foundation. Liu et al. [14] established a 2D train–bridge interaction model to investigate the vertical deflection and acceleration responses of the bridge based on an ETR500Y train. The dynamic model of the Sesia viaduct and the track system was established using finite element method. The primary suspension forces were directly solved according to the relative displacement between the wheel and the rail. The numerical simulation was validated by comparing the predicted accelerations and strains with measured results. Lou et al. [15] proposed a rail–bridge coupled element of unequal lengths, in which the length of a bridge element is longer than that of a rail element, to investigate the 2D dynamic problem of train–track–bridge interaction systems. They identified that a double-layer track model was more accurate than a single-layer track model and the mass of the sleeper had remarkable effect on the dynamic responses of the interactive system. It is evident that the cited research work only involved the 2D train–track–bridge interaction. On the other hand, the research on the three-dimensional (3D) train–track–bridge interaction has been less active. Wu et al. [16] developed a vehicle–rail–bridge interaction (VRBI) model for analysing the 3D dynamic interaction between moving trains and railway bridge. By using the dynamic condensation method, three types of vehicle–rail interaction (VRI) elements were derived. The 3D vibration of track was also taken into account. Aiming at the same problem raised in [14], Guo et al. [17] established a 3D dynamic analysis model for the spatial coupled train–bridge system. For the bridge subsystem a 3D rail–ballast–beam finite element model was created with consideration of the elasticity and the continuity of the track system. In addition, the same method used in [14] was adopted to solve the primary suspension forces. Tanabe et al. [18] built a 3D analysis model for the dimensional dynamic interaction between a Shinkansen train (bullet train) and railway structure. A non-linear spring element based on a trilinear elastic–plastic material model was devised to express the elastic–plastic behaviour of the parts in the structure, which is effective for solving practical problems.

With the rapid expansion of China's high-speed railway network in the twenty-first century, safety evaluation and design envelope of dynamic characteristics of various bridge structures are becoming increasingly important considerations particularly with the expansion of the high-speed railways at the 300–350 km/h operating speed. The essence of the considerations is the dynamic interactions among high-speed trains, tracks and bridges. As a result, the Railway Ministry of China in 2001 requested Zhai to lead a coordinated research group with participations from Southwest Jiaotong University, Beijing Jiaotong University, China Academy of Railway Sciences and Central South University to specifically study the high-speed train–track–bridge system dynamics, with the ultimate goal to provide an analytical methodology for simulating train passing bridge at high-speed operation. The result of the study was to be used for dynamic safety evaluation of new high-speed railway bridges. After the 10-year study, this goal has been achieved so as to meet the applicable need of China's high-speed railway bridge construction [19].

Based on the work by the team led by Zhai, this paper systematically introduces the framework for modelling and simulating high-speed train–track–bridge dynamic interactions, including the subsystem models and the interactivity models of the subsystems among the entire high-speed train–track–bridge system, including numerical solutions and computer simulation. Part II of the paper will present validation of the dynamic models and the software, as well as applications of the models in high-speed railway engineering in China.

2. Mechanism of high-speed train–track–bridge dynamic interaction

When a train passes a bridge, the train will induce vibration of the bridge and bring dynamic impact on the bridge structure, which can in reverse influence the running safety and the ride comfort of the train on the bridge. Obviously, the train and the bridge are essentially coupled with each other.

The train and bridge structure dynamically interact by virtue of the wheel–rail interaction as well as the track–bridge interaction. On the one hand, dynamic loads of vehicles are exerted on the rail, and transmitted downwards to sleepers (or track slabs) via fasteners and eventually delivered to the beam body. As a result, vibrations of track and bridge are induced. On the other hand, the vibration and deformation of the bridge affect the vibration of the track structure via the track–bridge interface, which causes the changes of the wheel–rail contact geometry and wheel–rail interactive forces. Once the wheel–rail forces vary, the dynamic behaviour of the vehicle system will be affected. Therefore, it could be concluded that the train, track and bridge have tight and substantial dynamic interactions. With the increase of train speed, the dynamic interactions of the train, the track and the bridge aggravate. Severe dynamic interactions will not only affect the operational safety of trains and the ride comfort of passengers passing through the bridge, but also have a direct influence on the bridge vibration as well which may affect its structural capability. Therefore, it is necessary to extend the study of high-speed train–bridge dynamic interaction into the investigation of high-speed train–track–bridge interaction so as to be able to get better understanding of the dynamic performance of the entire system.

Figure 1 illustrates the major elements and their relationships involving the high-speed train–track–bridge dynamic interactions. The entire system consists of three subsystems namely vehicle subsystem, track subsystem and bridge subsystem, which are coupled through the wheel–rail interaction and the track–bridge interaction,

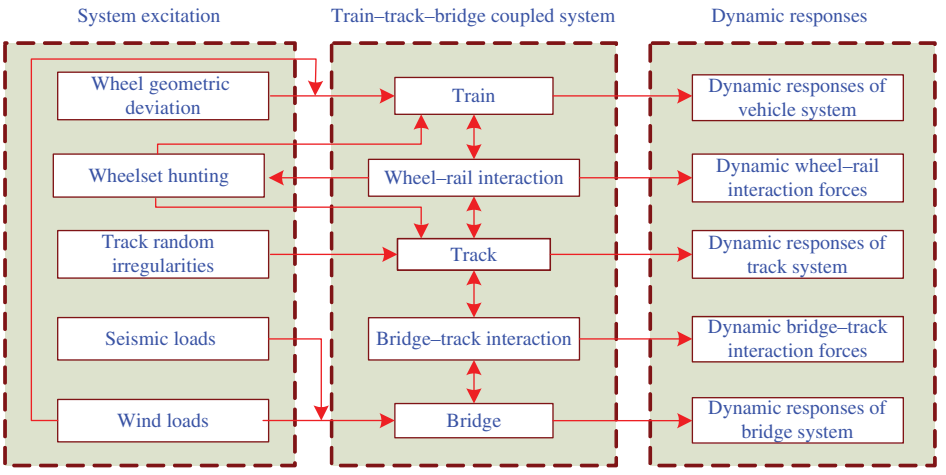

Figure 1. Elements of high-speed train–track–bridge dynamic interaction.

respectively. Under possible excitations such as track irregularities, non-round wheels and environmental wind loads, the train–track–bridge coupled system generate dynamic responses, including vehicle vibration responses, bridge structure dynamic responses, track vibration responses and wheel–rail dynamic forces. As a link connecting the train and the bridge, the wheel–rail dynamic interaction plays a crucial role in the coupled system.

3. High-speed train–track–bridge dynamic interaction model

A fundamental model of the high-speed train–track–bridge dynamic interaction can be established on the basis of the mechanism illustrated in Section 2. Although specific models for different high-speed trains or tracks and for different bridge structures can be very different, they all have the same basic framework, which takes into account the train, track, bridge subsystem components coupled with the wheel–rail interaction and the track–bridge interaction. As an example, Figure 2 shows the schematic diagram of a high-speed train–track–bridge dynamic interaction model for simply supported composite box-girder bridge with slab track structure on it. This is the typical beam type widely used in Chinese high-speed railway system, such as the Beijing–Shanghai high-speed railway and the Beijing–Guangzhou high-speed railway.

Compared with the early classic train–bridge vibration models, the high-speed train–track–bridge dynamic interaction model has the following unique characteristics. First, a wheel–rail spatially dynamic coupling model is introduced into the system to describe the wheel–rail interaction. Second, the vibration of track structure is considered in this model. Third, the subgrade–bridge transition sections are incorporated into the model in order to consider the dynamic effect of different support at both ends of the bridge. Field data shows that, when a train passes through the subgrade–bridge transition section rapidly, the running safety and the ride comport will be affected due to the sudden change of the under-rail supporting stiffness as well as the discrepant settlement of the subgrade. Thus, the current model is capable of realistically simulating the dynamic behaviour of the entire high-speed train–track–bridge system.

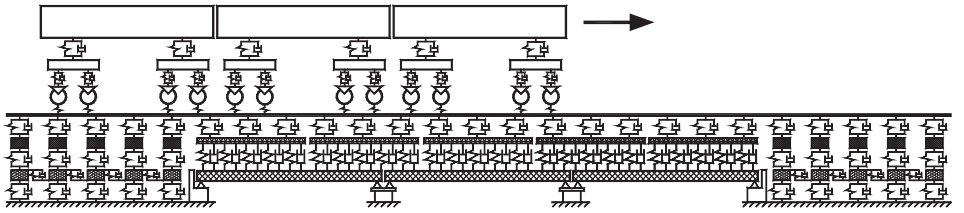

(a)

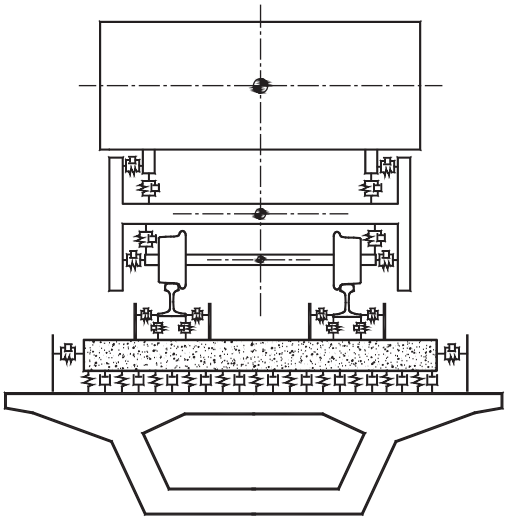

(b)

Figure 2. High-speed train–track–bridge dynamic interaction model: (a) side elevation; (b) end view.

3.1. *High-speed train model*

3.1.1. *Physical model*

The basic unit of a high-speed train model is the vehicle model, which depends on the specific train formation. In this paper, the vehicle submodel is established based on the multi-body system dynamics. It is assumed that:

(1) The car bodies, bogie frames and wheelsets are all rigid bodies with no elasticity.
(2) The train moves at a constant speed along the track without consideration of the stretching vibration of the vehicle and the longitudinal dynamic interaction between neighbouring vehicles.
(3) The car body is symmetrical about its centre of mass at *x*-, *y*- and *z*-directions.

As shown in Figures 3–5, the vehicle model of a high-speed train consists of seven rigid bodies, including the car body, bogies and wheelsets, as well as primary and secondary suspensions. The model thoroughly considers the linear or non-linear stiffness and damping properties of the primary and the secondary suspensions in three directions, e.g. non-linear yaw dampers and secondary lateral stop-block clearances [20]. Five

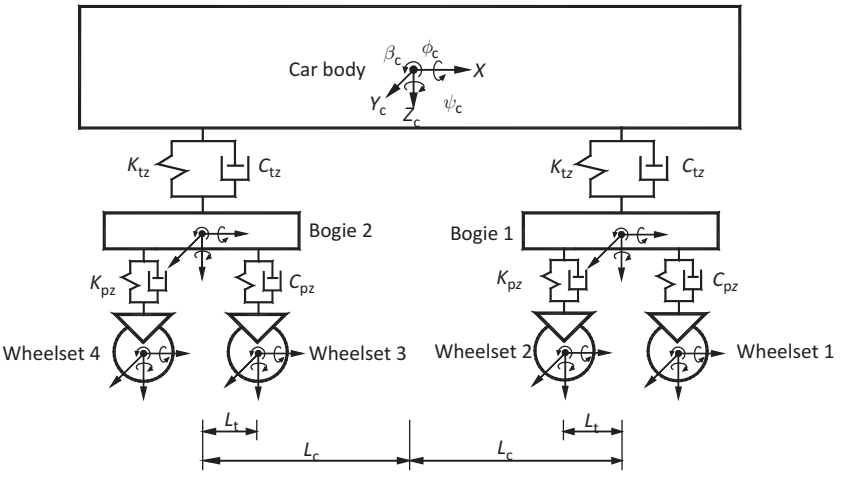

Figure 3. Three-dimensional high-speed vehicle model: side elevation.

degrees of freedom (DOFs) are taken into consideration for each rigid body, describing vertical, lateral, roll, yaw and pitch motions. In total, each vehicle model has 35 DOFs, as shown in Table 1.

3.1.2. *Equations of motion*

The equations of motion of the high-speed vehicle subsystem can be established according to the D'Alembert's principle, as shown in Equations (1)–(15), whose

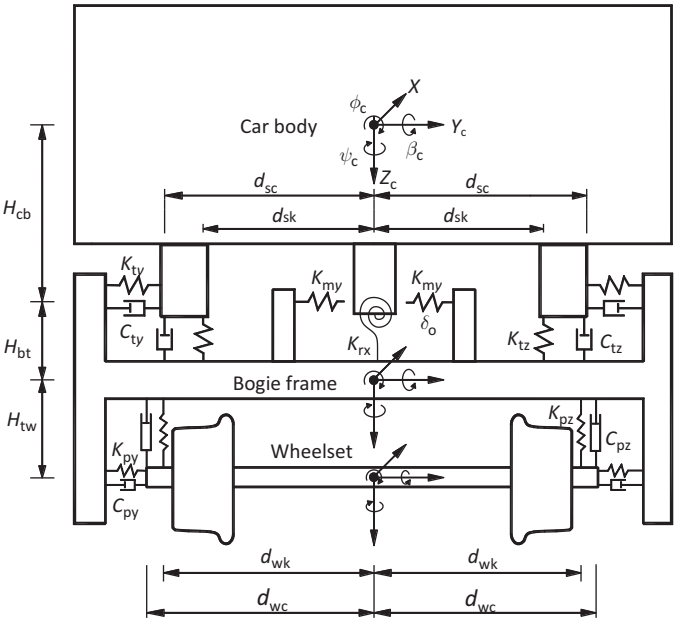

Figure 4. Three-dimensional high-speed vehicle model: end view.

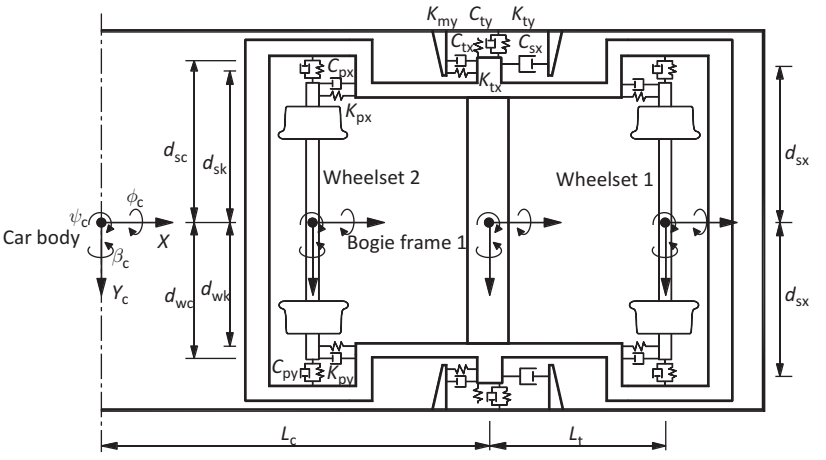

Figure 5. Three-dimensional high-speed vehicle model: plan view.

Table 1. Degrees of freedom of high-speed vehicle dynamic model.

Vehicle component	Lateral motion	Vertical motion	Roll motion	Yaw motion	Pitch motion
Car body	Y_c	Z_c	ϕ_c	ψ_c	β_c
Front bogie frame	Y_{t1}	Z_{t1}	ϕ_{t1}	ψ_{t1}	β_{t1}
Rear bogie frame	Y_{t2}	Z_{t2}	ϕ_{t2}	ψ_{t2}	β_{t2}
First wheelset	Y_{w1}	Z_{w1}	ϕ_{w1}	ψ_{w1}	β_{w1}
Second wheelset	Y_{w2}	Z_{w2}	ϕ_{w2}	ψ_{w2}	β_{w2}
Third wheelset	Y_{w3}	Z_{w3}	ϕ_{w3}	ψ_{w3}	β_{w3}
Fourth wheelset	Y_{w4}	Z_{w4}	ϕ_{w4}	ψ_{w4}	β_{w4}

notations are explained in Table 2. The vehicle suspension forces are dependent on the suspension properties as well as relative displacements and relative velocities between two components at the ends of the suspension systems. The wheelset forces are determined by the wheel–rail coupling model, which will be introduced in Section 3.4.

(1) Equations of motion of wheelsets (i = 1–4)

Vertical motion:

$$M_w\left(\ddot{Z}_{wi} - d_0\ddot{\phi}_{sewi} - \frac{V^2}{R_{wi}}\phi_{sewi}\right) = -F_{Lzi} - F_{Rzi} - N_{Lzi} - N_{Rzi} + F_{zfKLi} + F_{zfKRi} + F_{zfCLi} + F_{zfCRi} + M_w g \quad (1)$$

Lateral motion:

$$M_w\left(\ddot{Y}_{wi} + \frac{V^2}{R_{wi}} + r_0\ddot{\phi}_{sewi}\right) = -F_{yfLi} - F_{yfRi} + F_{Lyi} + F_{Ryi} + N_{Lyi} + N_{Ryi} + M_w g\phi_{sewi} \quad (2)$$

Table 2. Physical meaning of notations used in equations of motion of vehicle subsystem.

Notation	Physical meaning
$\phi_{\mathrm{sew}i}$	The superelevation angle of the curve high rail where the ith wheelset locates
$\phi_{\mathrm{set}i}$	The superelevation angle of the curve high rail where the ith bogie centre locates
ϕ_{sec}	The superelevation angle of the curve high rail where the car body centre locates
$R_{\mathrm{w}i}$	The curvature radius of the track where the ith wheelset locates
r_0	Nominal contact rolling radius of the wheel
$r_{\mathrm{L}i}$ and $r_{\mathrm{R}i}$	The left and right contact rolling radii of the ith wheel
Ω	Nominal rolling angular velocity of the wheel
$F_{\mathrm{L}xi}$, $F_{\mathrm{L}yi}$ and $F_{\mathrm{L}zi}$	The x-, y- and z-direction creep forces of the left wheel of the ith wheelset
$F_{\mathrm{R}xi}$, $F_{\mathrm{R}yi}$ and $F_{\mathrm{R}zi}$	The x-, y- and z-direction creep forces of the right wheel of the ith wheelset
$N_{\mathrm{L}xi}$, $N_{\mathrm{L}yi}$ and $N_{\mathrm{L}zi}$	The x-, y- and z-direction contact forces of the left wheel of the ith wheelset
$N_{\mathrm{R}xi}$, $N_{\mathrm{R}yi}$ and $N_{\mathrm{R}zi}$	The x-, y- and z-direction contact forces of the right wheel of the ith wheelset
$M_{\mathrm{L}xi}$, $M_{\mathrm{L}yi}$ and $M_{\mathrm{L}zi}$	The x-, y- and z-direction spin creep torque of the left wheel of the ith wheelset
$M_{\mathrm{R}xi}$, $M_{\mathrm{R}yi}$ and $M_{\mathrm{R}zi}$	The x-, y- and z-direction spin creep torque of the right wheel of the ith wheelset
$F_{x\mathrm{fL}i}$ and $F_{x\mathrm{fR}i}$	The left and right longitudinal forces at primary suspension of the ith wheelset
$F_{y\mathrm{fL}i}$ and $F_{y\mathrm{fR}i}$	The left and right lateral forces at primary suspension of the ith wheelset
$F_{z\mathrm{fKL}i}$ and $F_{z\mathrm{fKR}i}$	The left and right vertical spring forces at primary suspension of the ith wheelset
$F_{z\mathrm{fCL}i}$ and $F_{z\mathrm{fCR}i}$	The left and right vertical damping forces at primary suspension of the ith wheelset
$F_{x\mathrm{tL}i}$ and $F_{x\mathrm{tR}i}$	The left and right longitudinal forces at secondary suspension of the ith bogie
$F_{y\mathrm{tL}i}$ and $F_{y\mathrm{tR}i}$	The left and right lateral forces at secondary suspension of the ith bogie
$F_{z\mathrm{tKL}i}$ and $F_{z\mathrm{tKR}i}$	The left and right vertical spring forces at secondary suspension of the ith bogie
$F_{z\mathrm{tCL}i}$ and $F_{z\mathrm{tCR}i}$	The left and right vertical damping forces at secondary suspension of the ith bogie
$F_{x\mathrm{sL}i}$ and $F_{x\mathrm{sR}i}$	The left and right longitudinal forces at anti-hunting dampers of the ith bogie
$F_{y\mathrm{R}i}$	The lateral force of the stop-block on the ith bogie
$M_{\mathrm{R}i}$	Anti-roll torque of the ith bogie
d_0	Half of the distance between the left and right wheel–rail contact points

Roll motion:

$$\begin{aligned} I_{\mathrm{w}x}\left(\ddot{\phi}_{\mathrm{sew}i}+\ddot{\phi}_{\mathrm{w}i}\right)-I_{\mathrm{w}y}\left(\dot{\beta}_{\mathrm{w}i}-\Omega\right)\left(\dot{\psi}_{\mathrm{w}i}+\frac{V}{R_{\mathrm{w}i}}\right) &= d_0\left(F_{\mathrm{L}zi}+N_{\mathrm{L}zi}-F_{\mathrm{R}zi}-N_{\mathrm{R}zi}\right) \\ &\quad -r_{\mathrm{L}i}\left(F_{\mathrm{L}yi}+N_{\mathrm{L}yi}\right)-r_{\mathrm{R}i}\left(F_{\mathrm{R}yi}+N_{\mathrm{R}yi}\right) \\ &\quad +M_{\mathrm{L}xi}+M_{\mathrm{R}xi}+d_{\mathrm{wk}}\left(F_{z\mathrm{fKR}i}-F_{z\mathrm{fKL}i}\right) \\ &\quad +d_{\mathrm{wc}}\left(F_{z\mathrm{fCR}i}-F_{z\mathrm{fCL}i}\right) \end{aligned} \tag{3}$$

Yaw motion:

$$\begin{aligned} &I_{\mathrm{w}z}\left[\ddot{\psi}_{\mathrm{w}i}+V\frac{\mathrm{d}}{\mathrm{d}t}\left(\frac{1}{R_{\mathrm{w}i}}\right)\right]+I_{\mathrm{w}y}\left(\ddot{\phi}_{\mathrm{sew}i}+\ddot{\phi}_{\mathrm{w}i}\right)\left(\dot{\beta}_{\mathrm{w}i}-\Omega\right)=d_0\left(F_{\mathrm{L}xi}-F_{\mathrm{R}xi}\right) \\ &\quad +d_0\psi_{\mathrm{w}i}\left(F_{\mathrm{L}yi}+N_{\mathrm{L}yi}-F_{\mathrm{R}yi}-N_{\mathrm{R}yi}\right) \\ &\quad +M_{\mathrm{L}zi}+M_{\mathrm{R}zi}+d_{\mathrm{wk}}\left(F_{x\mathrm{fL}i}-F_{x\mathrm{fR}i}\right)+d_0\left(N_{\mathrm{L}xi}-N_{\mathrm{R}xi}\right) \end{aligned} \tag{4}$$

Rotation motion:

$$\begin{aligned} I_{\mathrm{w}y}\ddot{\beta}_{\mathrm{w}i} = {} & r_{\mathrm{R}i}F_{\mathrm{R}xi} + r_{\mathrm{L}i}F_{\mathrm{L}xi} + r_{\mathrm{R}i}\psi_{\mathrm{w}i}\left(F_{\mathrm{R}yi} + N_{\mathrm{R}yi}\right) + r_{\mathrm{L}i}\psi_{\mathrm{w}i}\left(F_{\mathrm{L}yi} + N_{\mathrm{L}yi}\right) + M_{\mathrm{L}yi} \\ & + M_{\mathrm{R}yi} + N_{\mathrm{L}xi}r_{\mathrm{L}i} + N_{\mathrm{R}xi}r_{\mathrm{R}i} \end{aligned} \tag{5}$$

(2) Equations of motion of bogie frames (i = 1, 2)

Vertical motion:

$$\begin{aligned} & M_{\mathrm{t}}\left[\ddot{Z}_{\mathrm{t}i} - d_0\ddot{\phi}_{\mathrm{set}i} - \frac{V^2}{R_{\mathrm{t}i}}\phi_{\mathrm{set}i}\right] = F_{z\mathrm{tKL}i} + F_{z\mathrm{tKR}i} + F_{z\mathrm{tCL}i} + F_{z\mathrm{tCR}i} + M_{\mathrm{t}}g \\ & - F_{z\mathrm{fKL}(2i-1)} - F_{z\mathrm{fKL}(2i)} - F_{z\mathrm{fCL}(2i-1)} - F_{z\mathrm{fCL}(2i)} \\ & - F_{z\mathrm{fKR}(2i-1)} - F_{z\mathrm{fKR}(2i)} - F_{z\mathrm{fCR}(2i-1)} - F_{z\mathrm{fCR}(2i)} \end{aligned} \tag{6}$$

Lateral motion:

$$\begin{aligned} & M_{\mathrm{t}}\left[\ddot{Y}_{\mathrm{t}i} + \frac{V^2}{R_{\mathrm{t}i}} + (r_0 + H_{\mathrm{tw}})\ddot{\phi}_{\mathrm{set}i}\right] = F_{y\mathrm{fL}(2i-1)} + F_{y\mathrm{f}L(2i)} - F_{y\mathrm{tL}i} + F_{y\mathrm{R}i} \\ & + F_{y\mathrm{fR}(2i-1)} + F_{y\mathrm{fR}(2i)} - F_{y\mathrm{tR}i} + M_{\mathrm{t}}g\phi_{\mathrm{set}i} \end{aligned} \tag{7}$$

Roll motion:

$$\begin{aligned} I_{\mathrm{t}x}\left[\ddot{\phi}_{\mathrm{t}i} + \ddot{\phi}_{\mathrm{set}i}\right] = {} & -\left(F_{y\mathrm{fL}(2i-1)} + F_{y\mathrm{fR}(2i-1)} + F_{y\mathrm{fL}(2i)} + F_{y\mathrm{fR}(2i)}\right)H_{\mathrm{tw}} \\ & + \left(F_{z\mathrm{fKL}(2i-1)} + F_{z\mathrm{fKL}(2i)} - F_{z\mathrm{fKR}(2i-1)} - F_{z\mathrm{fKR}(2i)}\right)d_{\mathrm{wk}} \\ & + \left(F_{z\mathrm{fCL}(2i-1)} + F_{z\mathrm{fCL}(2i)} - F_{z\mathrm{fCR}(2i-1)} - F_{z\mathrm{fCR}(2i)}\right)d_{\mathrm{wc}} \\ & + (F_{z\mathrm{tKR}i} - F_{z\mathrm{tKL}i})d_{\mathrm{sk}} + (F_{z\mathrm{tCR}i} - F_{z\mathrm{tCL}i})d_{\mathrm{sc}} \\ & - \left(F_{y\mathrm{tL}i} + F_{y\mathrm{tR}i} - F_{y\mathrm{R}i}\right)H_{\mathrm{bt}} + M_{\mathrm{R}i} \end{aligned} \tag{8}$$

Yaw motion:

$$\begin{aligned} I_{\mathrm{t}z}\left[\ddot{\psi}_{\mathrm{t}i} + V\frac{\mathrm{d}}{\mathrm{d}t}\left(\frac{1}{R_{\mathrm{t}i}}\right)\right] = {} & \left(F_{y\mathrm{fL}(2i-1)} + F_{y\mathrm{fR}(2i-1)} - F_{y\mathrm{fL}(2i)} - F_{y\mathrm{fR}(2i)}\right)l_{\mathrm{t}} \\ & + \left(F_{x\mathrm{fR}(2i-1)} + F_{x\mathrm{fR}(2i)} - F_{x\mathrm{fL}(2i-1)} - F_{x\mathrm{fL}(2i)}\right)d_{\mathrm{wk}} \\ & + (F_{x\mathrm{tL}i} - F_{x\mathrm{tR}i})d_{\mathrm{sk}} + (F_{x\mathrm{sL}i} - F_{x\mathrm{sR}i})d_{\mathrm{sx}} \end{aligned} \tag{9}$$

Pitch motion:

$$\begin{aligned} I_{\mathrm{t}y}\ddot{\beta}_{\mathrm{t}i} = {} & \left(F_{z\mathrm{fKL}(2i-1)} + F_{z\mathrm{fKR}(2i-1)} - F_{z\mathrm{fKL}(2i)} - F_{z\mathrm{fKR}(2i)}\right)l_{\mathrm{t}} \\ & + \left(F_{z\mathrm{fCL}(2i-1)} + F_{z\mathrm{fCR}(2i-1)} - F_{z\mathrm{fCL}(2i)} - F_{z\mathrm{fCR}(2i)}\right)l_{\mathrm{t}} \\ & - \left(F_{x\mathrm{fL}(2i-1)} + F_{x\mathrm{fR}(2i-1)} + F_{x\mathrm{fL}(2i)} + F_{x\mathrm{fR}(2i)}\right)H_{\mathrm{tw}} \\ & - (F_{x\mathrm{tL}i} + F_{x\mathrm{tR}i})H_{\mathrm{bt}} - (F_{x\mathrm{sL}i} + F_{x\mathrm{sR}i})H_{\mathrm{bt}} \end{aligned} \tag{10}$$

(3) Equations of motion of car body

Vertical motion:

$$M_{\mathrm{c}}\left[\ddot{Z}_{\mathrm{c}}-d_0\ddot{\phi}_{\mathrm{sec}}-\frac{V^2}{R_{\mathrm{c}}}\phi_{\mathrm{sec}}\right]=M_{\mathrm{c}}g-F_{z\mathrm{tKL1}}-F_{z\mathrm{tKR1}}-F_{z\mathrm{tKL2}}-F_{z\mathrm{tKR2}}-F_{z\mathrm{tCL1}}-F_{z\mathrm{tCR1}}-F_{z\mathrm{tCL2}}-F_{z\mathrm{tCR2}} \tag{11}$$

Lateral motion:

$$M_{\mathrm{c}}\left[\ddot{Y}_{\mathrm{c}}+\frac{V^2}{R_{\mathrm{c}}}+(r_0+H_{\mathrm{tw}}+H_{\mathrm{bt}}+H_{\mathrm{cb}})\ddot{\phi}_{\mathrm{sec}}\right]=M_{\mathrm{c}}g\phi_{\mathrm{sec}}-F_{y\mathrm{R1}}-F_{y\mathrm{R2}}+F_{y\mathrm{tL1}}+F_{y\mathrm{tL2}}+F_{y\mathrm{tR1}}+F_{y\mathrm{tR2}} \tag{12}$$

Roll motion:

$$\begin{aligned}I_{cx}\left[\ddot{\phi}_{\mathrm{c}}+\ddot{\phi}_{\mathrm{sec}}\right]=&-M_{\mathrm{R1}}-M_{\mathrm{R2}}-\left(F_{y\mathrm{tL1}}+F_{y\mathrm{tR1}}+F_{y\mathrm{tL2}}+F_{y\mathrm{tR2}}\right)H_{\mathrm{cb}}\\&+(F_{z\mathrm{tKL1}}+F_{z\mathrm{tKL2}}-F_{z\mathrm{tKR1}}-F_{z\mathrm{tKR2}})d_{\mathrm{sk}}\\&+(F_{z\mathrm{tCL1}}+F_{z\mathrm{tCL2}}-F_{z\mathrm{tCR1}}-F_{z\mathrm{tCR2}})d_{\mathrm{sc}}\\&+\left(F_{y\mathrm{R1}}+F_{y\mathrm{R2}}\right)H_{\mathrm{cb}}\end{aligned} \tag{13}$$

Yaw motion:

$$\begin{aligned}I_{\mathrm{cz}}\left[\ddot{\psi}_{\mathrm{c}}+V\frac{\mathrm{d}}{\mathrm{d}t}\left(\frac{1}{R_{\mathrm{c}}}\right)\right]=&\left(F_{y\mathrm{tL1}}+F_{y\mathrm{tR1}}-F_{y\mathrm{tL2}}-F_{y\mathrm{tR2}}\right)l_{\mathrm{c}}\\&+\left(F_{y\mathrm{R2}}-F_{y\mathrm{R1}}\right)l_{\mathrm{c}}+(F_{x\mathrm{tR1}}+F_{x\mathrm{tR2}}-F_{x\mathrm{tL1}}-F_{x\mathrm{tL2}})d_{\mathrm{sk}}\\&+(F_{x\mathrm{sR1}}+F_{x\mathrm{sR2}}-F_{x\mathrm{sL1}}-F_{x\mathrm{sL2}})d_{\mathrm{sx}}\end{aligned} \tag{14}$$

Pitch motion:

$$\begin{aligned}I_{\mathrm{cy}}\ddot{\beta}_{\mathrm{c}}=&(F_{z\mathrm{tKL1}}+F_{z\mathrm{tKR1}}-F_{z\mathrm{tKL2}}-F_{z\mathrm{tKR2}})l_{\mathrm{c}}+(F_{z\mathrm{tCL1}}+F_{z\mathrm{tCR1}}-F_{z\mathrm{tCL2}}-F_{z\mathrm{tCR2}})l_{\mathrm{c}}\\&-(F_{x\mathrm{tL1}}+F_{x\mathrm{tR1}}+F_{x\mathrm{tL2}}+F_{x\mathrm{tR2}})H_{\mathrm{cb}}-(F_{x\mathrm{sL1}}+F_{x\mathrm{sR1}}+F_{x\mathrm{sL2}}+F_{x\mathrm{sR2}})H_{\mathrm{cb}}\end{aligned} \tag{15}$$

3.2. *Track model*

There are two types of track structures laid on high-speed railway bridges: ballasted track and non-ballasted track. In China, the non-ballasted track structures are widely used on high-speed railway bridges. Among them, the slab track and the double-block non-ballasted track are common, e.g. in the Beijing–Tianjing intercity railway,

the Beijing–Shanghai high-speed railway and the Beijing–Guangzhou high-speed railway.

3.2.1. *Physical model*

For modelling the ballasted track structure on bridge, the method in [20] is adopted. The rails are treated as continuous Bernoulli–Euler beams and discretely supported at rail–sleeper junctions by rail pads, sleepers and ballasts, shown in Figure 6. In order to account for the continuity and the coupling effects of the interlocking ballast granules, a couple of shear stiffness (K_w) and shear damping (C_w) are introduced between adjacent ballast masses.

For the non-ballasted slab track laid on bridges, each slab can be modelled as a rectangle plate supported by a viscoelastic foundation, as described in [20].

For the double-block non-ballasted track, the track structure can be simply modelled as continuous rail beams discretely supported by fastenings (Figure 7). This is because the sleeper blocks are directly precast into the slab and there is no elasticity between the slab and the concrete base on the bridge deck.

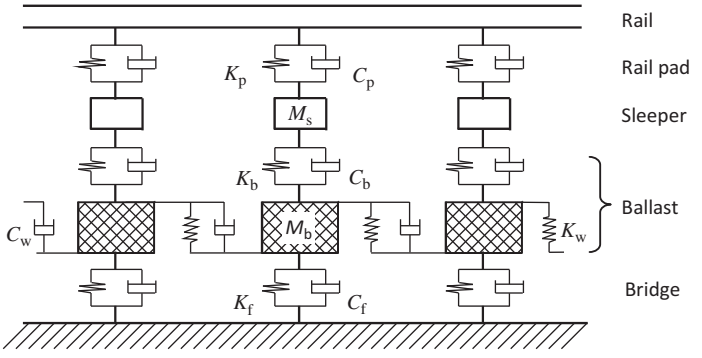

Figure 6. High-speed railway ballasted track model.

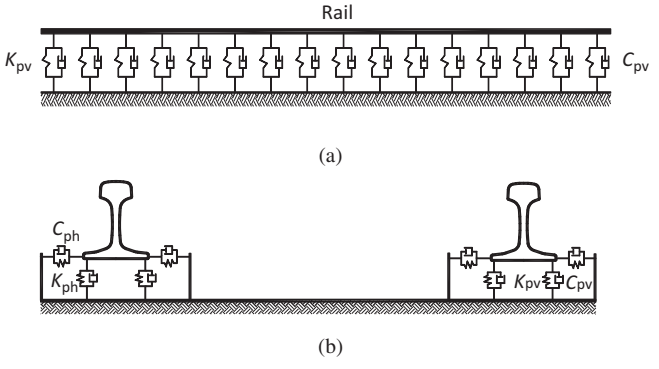

Figure 7. High-speed railway double-block non-ballasted track model: (a) side elevation; (b) end view.

3.2.2. *Equations of motion*

The equations of motion of the track subsystem are more complex than those of the vehicle subsystem due to the spatial continuity of the rails and the slabs. It is easy to establish the equations of motion of sleepers and ballast masses that are modelled as individual rigid bodies [21]. The equations of motion of the slabs could be found in [20].

Here are given the equations of motion of the rails in three vibrating directions:

Vertical vibration:

$$E_{\mathrm{r}}J_{\mathrm{r}y}\frac{\partial^4 z_{\mathrm{r}}(x,t)}{\partial x^4}+\rho_{\mathrm{r}}A_{\mathrm{r}}\frac{\partial^2 z_{\mathrm{r}}(x,t)}{\partial t^2}=-\sum_{i=1}^{N_{\mathrm{s}}}F_{\mathrm{rV}i}(t)\delta(x-x_{\mathrm{F}i})+\sum_{j=1}^{N_{\mathrm{w}}}P_j(t)\delta\big(x-x_{\mathrm{P}j}\big) \tag{16}$$

Lateral vibration:

$$E_{\mathrm{r}}J_{\mathrm{r}z}\frac{\partial^4 y_{\mathrm{r}}(x,t)}{\partial x^4}+\rho_{\mathrm{r}}A_{\mathrm{r}}\frac{\partial^2 y_{\mathrm{r}}(x,t)}{\partial t^2}=-\sum_{i=1}^{N_{\mathrm{s}}}F_{\mathrm{rL}i}(t)\delta(x-x_{\mathrm{F}i})+\sum_{j=1}^{N_{\mathrm{w}}}Q_j(t)\delta\big(x-x_{\mathrm{P}j}\big) \tag{17}$$

Torsional vibration:

$$\rho_{\mathrm{r}}J_{\mathrm{r}0}\frac{\partial^2 \phi_{\mathrm{r}}(x,t)}{\partial t^2}+G_{\mathrm{r}}J_{\mathrm{rt}}\frac{\partial^2 \phi_{\mathrm{r}}(x,t)}{\partial x^2}=-\sum_{i=1}^{N_{\mathrm{s}}}M_{\mathrm{F}i}(t)\delta(x-x_{\mathrm{F}i})+\sum_{j=1}^{N_{\mathrm{w}}}M_{\mathrm{W}j}(t)\delta\big(x-x_{\mathrm{P}j}\big) \tag{18}$$

The physical meaning of notations in Equations (16)–(18) is shown in Table 3.

Table 3. Physical meaning of notations used in equations of motion of rails.

Notation	Physical meaning
$z_{\mathrm{r}}(x,t)$	Vertical displacements of the rail
$y_{\mathrm{r}}(x,t)$	Lateral displacements of the rail
$\phi_{\mathrm{r}}(x,t)$	Torsional displacements of the rail
ρ_{r}	Rail mass density
A_{r}	Rail cross section area
E_{r}	Rail Young's modulus
G_{r}	Rail shearing modulus
$J_{\mathrm{r}y}$	Rail moment of inertia to the *y*-axle
$J_{\mathrm{r}z}$	Rail moment of inertia to the *z*-axle
$J_{\mathrm{r}0}$	Polar moment of inertia of the rail
J_{rt}	Torsional moment of inertia of the rail
$F_{\mathrm{rV}i}(t)$	Vertical dynamic force at the *i*th rail supporting point
$F_{\mathrm{rL}i}(t)$	Lateral dynamic force at the *i*th rail supporting point
$P_j(t)$	The *j*th wheel–rail vertical force
$Q_j(t)$	The *j*th wheel–rail lateral force
$M_{\mathrm{F}i}(t)$	Moment acting on the rail due to the *i*th fastener forces
$M_{\mathrm{W}j}(t)$	Moment acting on the rail due to the *j*th wheel–rail forces
$\delta(x)$	Dirac delta function
N_{s}	Number of the rail supporting points in calculated length
N_{w}	Number of the wheelsets in calculated length

In order to solve the fourth order partial differential equations of rails with time-stepping integration methods, it is necessary to transform Equations (16)–(18) into a series of second order ordinary differential equations in terms of the generalised coordinates. This could be achieved with the Ritz's method and results are given as follows:

$$\ddot{q}_{zk}(t)+\frac{E_{\mathrm{r}}J_{ry}}{\rho_{\mathrm{r}}A_{\mathrm{r}}}\left(\frac{k\pi}{l}\right)^4 q_{zk}(t)=-\sum_{i=1}^{N_{\mathrm{s}}}F_{\mathrm{rV}i}Z_k(x_{\mathrm{F}i})+\sum_{j=1}^{N_{\mathrm{w}}}P_jZ_k(x_{\mathrm{P}j})(k=1\sim N_{\mathrm{Z}}) \tag{19}$$

$$\ddot{q}_{yk}(t)+\frac{E_{\mathrm{r}}J_{rz}}{\rho_{\mathrm{r}}A_{\mathrm{r}}}\left(\frac{k\pi}{l}\right)^4 q_{yk}(t)=-\sum_{i=1}^{N_{\mathrm{s}}}F_{\mathrm{rL}i}Y_k(x_{\mathrm{F}i})+\sum_{j=1}^{N_{\mathrm{w}}}Q_jY_k(x_{\mathrm{P}j})(k=1\sim N_{\mathrm{Y}}) \tag{20}$$

$$\ddot{q}_{tk}(t)+\frac{G_{\mathrm{r}}J_{\mathrm{rt}}}{\rho_{\mathrm{r}}J_{\mathrm{r0}}}\left(\frac{k\pi}{l}\right)^2 q_{tk}(t)=-\sum_{i=1}^{N_{\mathrm{s}}}M_{\mathrm{F}i}\Phi_k(x_{\mathrm{F}i})+\sum_{j=1}^{N_{\mathrm{w}}}M_{\mathrm{W}j}\Phi_k(x_{\mathrm{P}j})(k=1\sim N_{\mathrm{T}}) \tag{21}$$

where l is the calculated length of the rail; $q_{zk}(t)$, $q_{yk}(t)$ and $q_{tk}(t)$ are the kth vertical, lateral and torsional mode time coordinates, respectively; and Z_k, Y_k and Φ_k are the rail vertical, lateral and torsional mode functions, described as

$$Z_k(x)=\sqrt{\frac{2}{\rho_{\mathrm{r}}A_{\mathrm{r}}l}}\sin\frac{k\pi x}{l} \tag{22}$$

$$Y_k(x)=\sqrt{\frac{2}{\rho_{\mathrm{r}}A_{\mathrm{r}}l}}\sin\frac{k\pi x}{l} \tag{23}$$

$$\Phi_k(x)=\sqrt{\frac{2}{\rho_{\mathrm{r}}J_{\mathrm{r0}}l}}\sin\frac{k\pi x}{l} \tag{24}$$

The rail vertical, lateral and torsional displacements at the time t can then be expressed as

$$z_{\mathrm{r}}(x,t)=\sum_{k=1}^{N_{\mathrm{Z}}}Z_k(x)q_{zk}(t) \tag{25}$$

$$y_{\mathrm{r}}(x,t)=\sum_{k=1}^{N_{\mathrm{Y}}}Y_k(x)q_{yk}(t) \tag{26}$$

$$\phi_{\mathrm{r}}(x,t) = \sum_{k=1}^{N_{\mathrm{T}}} \Phi_k(x) q_{tk}(t) \tag{27}$$

where N_{X}, N_{Y} and N_{T} are the total mode numbers of the rail vertical, lateral and torsional mode functions selected for the calculation.

3.3. *Bridge model*

The bridge structures are modelled with the finite element method. For different types of bridge structures, the spatial beam element, the spatial pole element, the plate element and other special elements are used for modelling specific components. Therefore, a complete bridge model can be established in detail, including the girders, the piers, the frusta foundation and other appurtenances. An example of the finite element model for a large complicated bridge in actual railway engineering will be presented in the second part of the paper.

3.4. *Wheel–rail dynamic interaction model*

3.4.1. *Wheel–rail dynamic coupling model*

Conventional dynamic analyses of train and bridge system are usually based on the assumption that the displacement of a wheel is always equal to that of the bridge beam under the wheel. In fact, the track structure laid on the bridge is an elastic-damping system. On account of the wheel load-induced vertical and lateral vibrations and deformations of the track structure, the displacements of the wheel and the underneath bridge are unequal. On the other hand, when vehicles move on an irregular track with high speed, three types of wheel–rail contact states shown in Figure 8 are possible. In some specific conditions, the instantaneous loss of contact between one side wheel of a wheelset and the rail may occur; and worse, it may happen to both sides of the wheelset as in Figure 8(c).

In order to make the description of wheel–rail dynamic interaction more accurate and reasonable, a spatially dynamic wheel–rail coupling model previously proposed by the author [20,22] is adopted in this paper, as in Figure 9. Unlike the classical wheel–rail contact model, in which the rails are assumed to be fixed without any movement, the model presented here is capable of considering three kinds of rail motions in vertical, lateral and torsional directions, and the situation of a wheel losing its contact with the rail. Therefore, the model is suitable for evaluating the dynamic behaviour of high-speed trains passing through bridges in an integrated and complete manner.

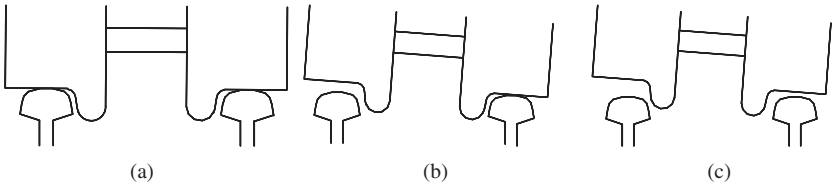

Figure 8. Wheel–rail contact states: (a) constant contact, (b) instantaneous loss of contact at one side and (c) loss of contact at two sides.

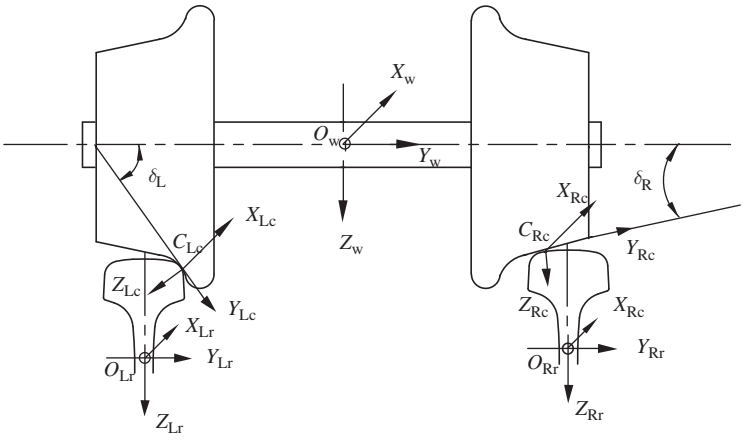

Figure 9. Wheel–rail dynamic coupling model.

3.4.2. *Calculation of wheel–rail normal contact forces*

The non-linear Hertzian elastic contact theory is used to calculate the wheel–rail normal contact forces:

$$P_{\mathrm{N}}(t) = \left[\frac{1}{G}\delta N(t)\right]^{3/2} \tag{28}$$

where G is the wheel–rail contact constant; $\delta N(t)$ is the wheel–rail normal elastic compression deformation. The left and right wheel–rail normal elastic compression deformation δN_{L} and δN_{R} can be expressed as

$$\begin{cases} \delta N_{\mathrm{L}} = \dfrac{\delta Z_{\mathrm{L}}}{\cos(\delta_{\mathrm{L}} + \phi_{\mathrm{w}})} \\ \delta N_{\mathrm{R}} = \dfrac{\delta Z_{\mathrm{R}}}{\cos(\delta_{\mathrm{R}} - \phi_{\mathrm{w}})} \end{cases} \tag{29}$$

where δ_{L} and δ_{R} are the left and right wheel–rail contact angles, respectively; ϕ_{w} denotes the wheelset roll angle; δZ_{L} and δZ_{R} are the left and right wheel–rail vertical relative displacements, which depend on the motion of wheelset and rail and the wheel–rail contact state.

Obviously, when δZ_{L} or δZ_{R} is less than zero indicating that the wheel at left or right side separates from the rail, the left or right side wheel–rail normal contact force is then equal to zero.

3.4.3. *Calculation of tangential wheel–rail creep forces*

Based on the Kalker's linear creep theory [23], the wheel–rail longitudinal creep force F_x, the lateral creep force F_y and the spin creep torque M_z can be described by

$$\begin{cases} F_x = -f_{11}\xi_x \\ F_y = -f_{22}\xi_y - f_{23}\xi_{sp} \\ M_z = f_{23}\xi_y - f_{33}\xi_{sp} \end{cases} \tag{30}$$

where f_{ij} represents the creep coefficients and the definitions of the longitudinal, lateral and spin creepage ξ_x, ξ_y and ξ_{sp} are as follows:

$$\begin{cases} \xi_x = \frac{V_{w1}-V_{r1}}{V} \\ \xi_y = \frac{V_{w2}-V_{r2}}{V} \\ \xi_{sp} = \frac{\Omega_{w3}-\Omega_{r3}}{V} \end{cases} \tag{31}$$

in which V_{w1}, V_{w2} and Ω_{w3} are the longitudinal, lateral and spin speeds of the wheel at contact point, respectively; V_{r1}, V_{r2} and Ω_{r3} are the speeds of the rail at the contact point and V is the wheelset speed moving on rails.

Since the Kalker's linear creep theory is only suited to the cases with small creepages, the non-linear modification should be made, for example, by Shen–Hedrick–Elkins model [24], for the situations of large creepages.

3.5. *Track–bridge dynamic interaction model*

Track–bridge dynamic interaction models are established to determine the track–bridge interaction forces. In this paper, the track–bridge interaction is discretised into a series of point-to-point interactions which are connected with linear spring and damping at each contact point. Both ballasted track–bridge dynamic interaction model and non-ballasted track–bridge dynamic interaction model are introduced.

Figure 10 is the schematic diagram of the ballasted track–bridge dynamic interaction model, in which the ballast has direct contact to the bridge deck.

It can be seen from the track–bridge relations shown in Figure 10 that the left and right vertical ballast–bridge interaction forces F_{sbVLi} and F_{sbVRi} under the ith sleeper can be expressed by

$$\begin{cases} F_{sbVLi} = K_{fV}(z_{bLi} - z_{bV} + \phi_b d) + C_{fV}\left(\dot{z}_{bLi} - \dot{z}_{bV} + \dot{\phi}_b d\right) \\ F_{sbVRi} = K_{fV}(z_{bRi} - z_{bV} - \phi_b d) + C_{fV}\left(\dot{z}_{bRi} - \dot{z}_{bV} - \dot{\phi}_b d\right) \end{cases} \tag{32}$$

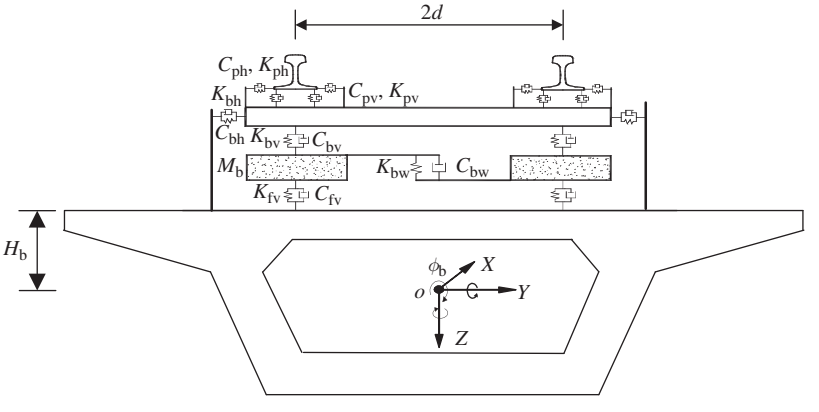

Figure 10. Ballasted track–bridge dynamic interaction model.

where K_{fv} and C_{fv} are the vertical stiffness and damping of the ballast; $z_{\mathrm{bL}i}$ and $z_{\mathrm{bR}i}$ are the vertical displacements of the ballast under the left and right rails, respectively; z_{bv} and ϕ_{b} are the vertical displacement and the rotation angle of the centroid O of the bridge section; d denotes half the gauge.

The lateral ballast–bridge interaction forces $F_{\mathrm{sbH}i}$ is determined by the lateral ballast resistance between sleeper and bridge, which can be described as

$$F_{\mathrm{sbH}i} = K_{\mathrm{bh}}(y_{\mathrm{sl}i} - y_{\mathrm{bh}} - \phi_{\mathrm{b}}H_{\mathrm{b}}) + C_{\mathrm{bh}}\left(\dot{y}_{\mathrm{sl}i} - \dot{y}_{\mathrm{bh}} - \dot{\phi}_{\mathrm{b}}H_{\mathrm{b}}\right) \tag{33}$$

where K_{bh} and C_{bh} are the lateral stiffness and damping of the ballast between the sleeper and the bridge, respectively. $y_{\mathrm{sl}i}$ denotes the lateral displacement of the ith sleeper; y_{bh} is the lateral displacement of the centroid O and H_{b} is the height from the centroid O to bridge deck.

For the non-ballasted track, the slab track–bridge dynamic interaction model is taken as an example, shown in Figure 11.

The lateral track–bridge interaction forces $F_{\mathrm{sH}i}$ at the ith support section and the vertical track–bridge interaction forces $F_{\mathrm{sV}ij}$ at the jth support point are calculated by

$$\begin{cases} F_{\mathrm{sH}i} = K_{\mathrm{sh}}(y_{\mathrm{s}i} - y_{\mathrm{bh}} - \phi_{\mathrm{b}}H_{\mathrm{b}}) + C_{\mathrm{sh}}\left(\dot{y}_{\mathrm{s}i} - \dot{y}_{\mathrm{bh}} - \dot{\phi}_{\mathrm{b}}H_{\mathrm{b}}\right) \\ F_{\mathrm{sV}ij} = K_{\mathrm{sv}}\left(z_{\mathrm{s}ij} - z_{\mathrm{bv}} + \phi_{\mathrm{b}}x_{\mathrm{s}ij}\right) + C_{\mathrm{sv}}\left(\dot{z}_{\mathrm{s}ij} - \dot{z}_{\mathrm{bv}} + \dot{\phi}_{\mathrm{b}}x_{\mathrm{s}ij}\right) \end{cases} \tag{34}$$

where K_{sh} and C_{sh} represent the lateral stiffness and damping of track slab, respectively; K_{sv} and C_{sv} denote the stiffness and damping of elastic layer under the track slab including the concrete–asphalt (CA) mortar and/or the rubber pad; $y_{\mathrm{s}i}$ is the lateral displacement of the slab; $z_{\mathrm{s}ij}$ is the vertical displacement of the slab at the jth support point and $x_{\mathrm{s}ij}$ represents the lateral distance between the bridge section centroid and the jth support point of the ith support section under the slab.

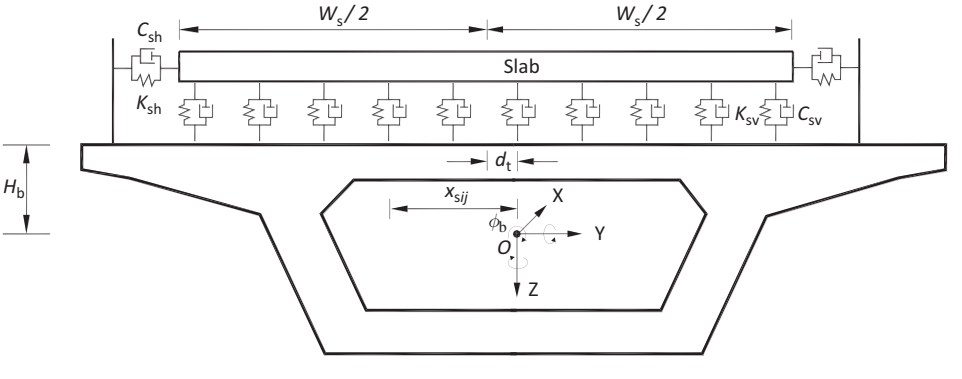

Figure 11. Slab track–bridge dynamic interaction model.

4. Numerical simulation of high-speed train–track–bridge system dynamics

Computer simulation of the high-speed train–track–bridge system dynamics provides an efficient and effective approach to evaluating the running safety of trains and the ride comfort of passengers passing through bridges at various high speeds.

4.1. *Numerical integration scheme*

Since the high DOFs of the high-speed train–track–bridge dynamic system as well as the strong non-linearities and high frequencies arising from the wheel–rail contact all contribute to the complexity of the model, it is crucial to seek a high-efficiency numerical algorithm to solve the dynamic responses for such a large-scale system.

After aborative comparison of different time-integration methods, a hybrid explicit–implicit integration scheme is eventually proposed. The simple fast explicit two-step integration method previously put forward by Zhai [25] is adopted to solve the train–track system dynamics, while the Newmark-β implicit integration method [26] is employed for analysis of the bridge structure dynamics. It has been proved that the Zhai method is computationally fast and therefore efficient for dynamic analyses of the vehicle-track coupled system with strong non-linearities [20], and the Newmark-β method is suitable for complex structure dynamics analysis. Numerical integration processes for the train–track system and for the bridge system are harmonised through the track–bridge interaction. Numerical calculation has shown the effectiveness of the hybrid explicit–implicit scheme.

The basic principle of Zhai's explicit two-step method is as follows: the displacements and velocities of a system at next time step ($t = (n+1)\Delta t$) can be estimated based on the dynamic responses at previous two steps ($t = n\Delta t$, $t = (n-1)\Delta t$), and the accelerations at time step $t = (n+1)\Delta t$ are calculated from the equations of motion. The integration scheme to calculate the displacement and the velocity of a system is expressed as [25]

$$\begin{cases} \mathbf{u}_{n+1} = \mathbf{u}_n + \dot{\mathbf{u}}_n \Delta t + (1/2 + \psi)\ddot{\mathbf{u}}_n \Delta t^2 - \psi \ddot{\mathbf{u}}_{n-1} \Delta t^2 \\ \dot{\mathbf{u}}_{n+1} = \dot{\mathbf{u}}_n + (1+\varphi)\ddot{\mathbf{u}}_n \Delta t - \varphi \ddot{\mathbf{u}}_{n-1} \Delta t \end{cases} \tag{35}$$

where $\mathbf{u}$, $\dot{\mathbf{u}}$ and $\ddot{\mathbf{u}}$ are the generalised displacement, velocity and acceleration of the system, respectively; Δt is the time step; φ and ψ are free parameters that control the stability and numerical dissipation of the algorithm. Usually, a value of 1/2 could be assigned to φ and ψ to achieve good compatibility between numerical stability and accuracy.

Substituting Equation (35) into the equations of motion of both vehicle subsystem and track subsystem at time step $t = (n+1)\Delta t$:

$$\mathbf{M}_{\mathrm{v}} \ddot{\mathbf{u}}_{\mathrm{v},n+1} + \mathbf{C}_{\mathrm{v}} \dot{\mathbf{u}}_{\mathrm{v},n+1} + \mathbf{K}_{\mathrm{v}} \mathbf{u}_{\mathrm{v},n+1} = \mathbf{R}_{\mathrm{v},n+1} \tag{36}$$

$$\mathbf{M}_{\mathrm{t}} \ddot{\mathbf{u}}_{\mathrm{t},n+1} + \mathbf{C}_{\mathrm{t}} \dot{\mathbf{u}}_{\mathrm{t},n+1} + \mathbf{K}_{\mathrm{t}} \mathbf{u}_{\mathrm{t},n+1} = \mathbf{R}_{\mathrm{t},n+1} \tag{37}$$

yields

$$\ddot{\mathbf{u}}_{\mathrm{v},n+1} = \mathbf{M}_{\mathrm{v}}{}^{-1}\tilde{\mathbf{R}}_{\mathrm{v},n+1} \tag{38}$$

$$\ddot{\mathbf{u}}_{\mathrm{t},n+1} = \mathbf{M}_{\mathrm{t}}{}^{-1}\tilde{\mathbf{R}}_{\mathrm{t},n+1} \tag{39}$$

where

$$\begin{aligned}\tilde{\mathbf{R}}_{\mathrm{v},n+1} = {} & \mathbf{R}_{\mathrm{v},n+1} - \mathbf{K}_{\mathrm{v}}\mathbf{u}_{\mathrm{v},n} - [\mathbf{C}_{\mathrm{v}} + \mathbf{K}_{\mathrm{v}}\Delta t]\dot{\mathbf{u}}_{\mathrm{v},n} \\ & - [(1+\varphi)\mathbf{C}_{\mathrm{v}} + (1/2+\psi)\mathbf{K}_{\mathrm{v}}\Delta t]\ddot{\mathbf{u}}_{\mathrm{v},n}\Delta t + [\varphi\mathbf{C}_{\mathrm{v}} + \psi\mathbf{K}_{\mathrm{v}}\Delta t]\ddot{\mathbf{u}}_{\mathrm{v},n-1}\Delta t\end{aligned} \tag{40}$$

$$\begin{aligned}\tilde{\mathbf{R}}_{\mathrm{t},n+1} = {} & \mathbf{R}_{\mathrm{t},n+1} - \mathbf{K}_{\mathrm{t}}\mathbf{u}_{\mathrm{t},n} - [\mathbf{C}_{\mathrm{t}} + \mathbf{K}_{\mathrm{t}}\Delta t]\dot{\mathbf{u}}_{\mathrm{t},n} \\ & - [(1+\varphi)\mathbf{C}_{\mathrm{t}} + (1/2+\psi)\mathbf{K}_{\mathrm{t}}\Delta t]\ddot{\mathbf{u}}_{\mathrm{t},n}\Delta t + [\varphi\mathbf{C}_{\mathrm{t}} + \psi\mathbf{K}_{\mathrm{t}}\Delta t]\ddot{\mathbf{u}}_{\mathrm{t},n-1}\Delta t\end{aligned} \tag{41}$$

In above equations, $\mathbf{M}_{\mathrm{v}}$, $\mathbf{C}_{\mathrm{v}}$, $\mathbf{K}_{\mathrm{v}}$, $\mathbf{R}_{\mathrm{v}}$ and $\mathbf{M}_{\mathrm{t}}$, $\mathbf{C}_{\mathrm{t}}$, $\mathbf{K}_{\mathrm{t}}$, $\mathbf{R}_{\mathrm{t}}$ are the mass matrices, damping matrices, stiffness matrices and generalised load vector matrices of the vehicle subsystem and track subsystem, respectively.

Based on the initial conditions of the vehicle subsystem $\mathbf{u}_{\mathrm{v},0}$ and $\dot{\mathbf{u}}_{\mathrm{v},0}$, as well as the track subsystem $\mathbf{u}_{\mathrm{t},0}$ and $\dot{\mathbf{u}}_{\mathrm{t},0}$, the procedure of the integration is performed in accordance with the formulas (35), (38) and (39). Combined with the wheel–rail contact forces obtained from the wheel–rail interaction model, the system dynamic responses including displacements, velocities and accelerations at each time step can be calculated recursively.

Because the mass matrices $\mathbf{M}_{\mathrm{v}}$ and $\mathbf{M}_{\mathrm{t}}$ are usually diagonal matrices, no algebraic equations have to be solved to obtain the inverse mass matrices required in Equations (38) and (39) at each time step. Therefore, the computational efficiency is greatly enhanced.

4.2. *Dynamic simulation software TTBSIM of the train–track–bridge system*

On the basis of the discussed high-speed train–track–bridge interaction model and the numerical integration scheme, a large-scale dynamic simulation software named the train–track–bridge interaction simulation software (TTBSIM) was jointly developed by Southwest Jiaotong University, Beijing Jiaotong University, China Academy of Railway Sciences and Central South University.

The TTBSIM software consists of five modules, including three basic modules for train, track and bridge, respectively, and two coupling modules describing subsystem interactions. The train module is coupled with the track module through the wheel–rail interaction module, while the track module and the bridge one are connected by the track–bridge interaction module.

Figure 12 shows the flow chart of the TTBSIM simulation system. Database of train, track, bridge and track irregularities are included as input data. Displacements and velocities of each degree of freedom can be acquired by means of the time-integration methods. Dynamic forces between wheel and rail and between track and bridge are ascertained through the wheel–rail interaction model and the track–bridge interaction model, respectively. Accelerations of each degree of freedom are calculated from the equations of motion of each subsystem. The whole time history of the system can be obtained step by step with a specified time step.

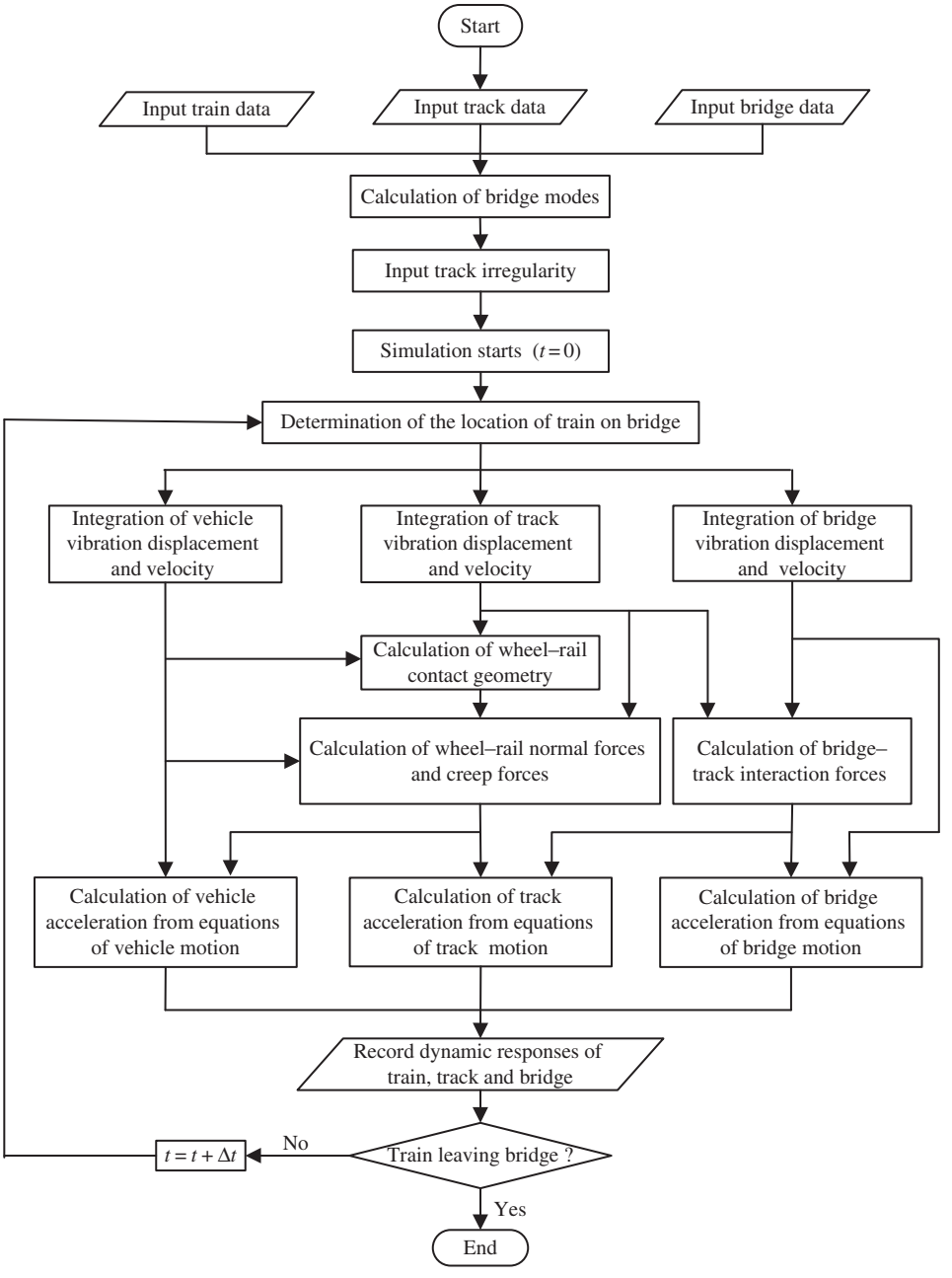

Figure 12. Flow chart of the TTBSIM simulation software.

Dynamic simulation of the complete train–track–bridge system involving variations of train formation, operating speed, track structure and bridge structure can be carried out with the TTBSIM software. Dynamic responses of train, track, bridge subsystems and the interfaces between each of the two subsystems can be obtained, such as vehicle vibration accelerations, vertical and lateral wheel–rail forces, rail pad forces, track structure

vibration displacements and accelerations, the natural frequencies of bridge structure, vertical deflections and lateral amplitudes of beam, bridge accelerations and impact coefficient. Based on these dynamic responses, a synthetic evaluation of dynamic performance of the bridge as well as the operational safety and the ride comfort can be performed.

5. Conclusions

A framework for modelling and simulation of high-speed train–track–bridge dynamic interactions is presented in the paper. A fundamental model has been established for analysis of the train–track–bridge dynamic interactions, including the high-speed vehicle model, the ballasted and non-ballasted track models, the bridge model, as well as the wheel–rail interaction model and the track–bridge interaction model. Dynamic responses of such a large system are solved numerically with an explicit–implicit integration scheme in the time domain. On the basis of the models and the numerical algorithms, a computation software named TTBSIM has been developed to simulate the dynamic performances of the overall train–track–bridge system, including the train running safety and the ride comfort of passengers, the dynamic behaviour of track structures and the dynamic performances of bridges. These features are useful for safety assessment of newly designed high-speed railway bridges.

The model validation and applications of the TTBSIM software for high-speed railway bridges will appear in Part II of the paper.

Acknowledgements

This research was supported by National Basic Research Program of China (973 Program) under grants 2013CB036206 and 2013CB036203, by National Natural Science Foundation of China (NSFC) under grant 50838006 and by the Science and Technology Research Program of Chinese Ministry of Railways under grant 2001G40. The authors would like to thank all the collaborators of this multi-disciplinary research project.

References

[1] Timoshenko S. On the forced vibrations of bridges. Philos Mag Ser. 1922;43:1018–1019.
[2] Mise K, Kunii S. A theory for the forced vibration of a railway bridge under the action of moving loads. Q J Mech Appl Math. 1956;9:195–206.
[3] Frýba L. Dynamics of railway bridges. London: Thomas Telford; 1996.
[4] Chu KH, Garg VK, Wiriyachi A. Dynamic interaction of train and bridge. Veh Syst Dyn. 1980;9(4):207–236.
[5] Bhatti MH. Vertical and lateral dynamic response of railway bridge due to nonlinear vehicle and track irregularities [PhD dissertation]. Chicago: Illinois Institute of Technology; 1982.
[6] Diana G, Cheli F. Dynamic interaction of railway systems with large bridges. Veh Syst Dyn. 1989;18(1–3):71–106.
[7] Bogaert V. Dynamic response of trains crossing large span double-track bridges. J Constructional Steel Res. 1993;24(1):57–74.
[8] Zhai WM, Sun X. A detailed model for investigating vertical interaction between railway vehicle and track. Veh Syst Dyn. 1994;23(Suppl):603–615.
[9] Cai CB, Zhai WM. Dynamic analysis of vertically coupled locomotive–track–bridge system. J Southwest Jiaotong Univ [in Chinese]. 1997;32(6):628–632.
[10] Zhai WM, Cai CB. Train/track/bridge dynamic interactions: simulation and applications. Veh Syst Dyn. 2002;37(Suppl):653–665.

[11] Zhai WM, Cai CB, Wang KY. Numerical simulation and field experiment of high-speed train–track–bridge system dynamics. Veh Syst Dyn. 2004;41(Suppl):677–686.
[12] Cheng YS, Au FTK, Cheung YK. Vibration of railway bridges under a moving train by using bridge–track–vehicle element. Eng Struct. 2001;23:1597–1606.
[13] Biondi B, Muscolino G, Sofi A. A substructure approach for dynamic analysis of train–track–bridge system. Comput Struct. 2005;83:2271–2281.
[14] Liu K, Reynders E, De Roeck G, Lombaert G. Experimental and numerical analysis of a composite bridge for high-speed trains. J Sound Vib. 2009;320:201–220.
[15] Lou P, Yu ZW, Au FTK. Rail–bridge coupling element of unequal lengths for analyzing train–track–bridge interaction systems. Appl Math Model. 2012;36:1395–1414.
[16] Wu YS, Yang YB, Yau JD. Three-dimensional analysis of train–rail–bridge interaction problems. Veh Syst Dyn. 2001;36(1):1–35.
[17] Guo WW, Xia H, De Roeck G, Liu K. Integral model for train–track–bridge interaction on the Sesia viaduct: dynamic simulation and critical assessment. Comput Struct. 2012;112–113: 205–216.
[18] Tanabe M, Wakui H, Matsumoto N, Okuda H, Sogabe M, Komiya S. Computational model of a Shinkansen train running on the railway structure and the industrial applications. J Mater Process Technol. 2003;140:705–710.
[19] Zhai WM, Xia H. Train–track–bridge dynamic interaction: theory and engineering application [in Chinese]. Beijing: Science Press; 2011.
[20] Zhai WM, Wang KY, Cai CB. Fundamentals of vehicle–track coupled dynamics. Veh Syst Dyn. 2009;47(11):1349–1376.
[21] Zhai WM, Cai Z. Dynamic interaction between a lumped mass vehicle and a discretely supported continuous rail track. Comput Struct. 1997;63(5):987–997.
[22] Chen G, Zhai WM. A new wheel/rail spatially dynamic coupling model and its verification, Veh Syst Dyn. 2004;41(4):301–322.
[23] Kalker JJ. On the rolling contact of two elastic bodies in the presence of dry friction [PhD dissertation]. Netherlands: Delft University of Technology; 1967.
[24] Shen ZY, Hedrick JK, Elkins JA. A comparison of alternative creep force models for rail vehicle dynamic analysis. Proceedings of 8th IAVSD Symposium; Cambridge: MIT; 1983 June. p. 591–605.
[25] Zhai WM. Two simple fast integration methods for large-scale dynamic problems in engineering. Int J Numer Methods Eng. 1996;39(24):4199–4214.
[26] Newmark NM. A method of computation for structural dynamics. J Eng Mech Div. ASCE. 1959;85(2):67–94.